special case of $M_1 = M_2$, $V = V_1w_1 + V_2w_2$ (the rule of volume additivity is satisfied). When M_1 is not equal to M_2, the rule of volume additivity is not satisfied. It is caused by a difference of the molecular weights of the comonomers.
(19) Krause, S. *J. Macromol. Sci., Rev. Macrmol. Chem.* **1972**, *C7* (2), 251.
(20) Scott, R. L. *J. Chem. Phys.* **1949**, *17*, 279.
(21) Hildebrand, J. H.; Scott, R. L. *The Solubility of Nonelectrolytes*, 3rd ed.; Reinhold: New York, 1950.
(22) Kressler, J.; Kammer, H. W.; Klostermann, K. *Polym. Bull.* **1986**, *15*, 113.
(23) Hoy, K. L. *J. Paint Technol.* **1970**, *42*, 76.

Blend Miscibility of Bisphenol A Polycarbonate and Poly(ethylene terephthalate) As Studied by Solid-State High-Resolution ^{13}C NMR Spectroscopy

P. Mark Henrichs,* John Tribone, and Dennis J. Massa

Corporate Research Laboratories—Eastman Kodak Company, Rochester, New York 14650

James M. Hewitt

Analytical Technology Division—Eastman Kodak Company, Rochester, New York 14650.

Received November 20, 1987

ABSTRACT: Blends of poly(ethylene terephthalate) (PET) and bisphenol A polycarbonate (BPAPC), cast as films from solution in a mixture of hexafluoro-2-propanol and dichloromethane, pressed as a film, and then quenched in ice water, were examined with solid-state high-resolution ^{13}C NMR spectroscopy and differential scanning calorimetry. As prepared, the samples contained separated domains of amorphous PET and BPAPC exceeding 150 Å in size. Heating to 265 °C for about 4 min, followed by cooling in air or in a metal heating block, resulted in crystallization of part of the PET. Further heating and cooling cycles resulted in degradation of the size of the PET crystals while fragments derived from PET were mixed at the molecular level with those derived from BPAPC. The homogenization process apparently occurred as a result of chemical reactions that included the partial loss of the BPAPC carbonyl and a loss of symmetry of the ethylene glycol moiety of PET.

Introduction

Traditional wisdom asserts that polymers of different chemical composition are miscible at the molecular level only in isolated cases. The entropy of mixing that leads to miscibility of many compounds composed of small molecules is essentially absent for high-molecular-weight polymers.

The realization in recent years that, in practice, a great many polymer pairs do form homogeneous blends has stirred considerable interest. The simple fact that the composition of such polymer blends can be varied by the chemist provides a new level of control of polymer properties. Unfortunately, the reasons why some pairs of polymers mix uniformly while other, apparently similar materials, do not is not completely understood. Progress has been made toward development of appropriate theories,[1-7] but additional experimental results on which to base such theories are still needed.

There have been a number of reports that various kinds of polyesters form homogeneous blends with bisphenol A polycarbonate.[8-14] In many cases specific properties of such blends have been measured.[15-21] Thermoplastics containing polyester/polycarbonate blends have a large potential market in automobile parts.

Unfortunately, the early reports that many polyesters are miscible with polycarbonates have not always been supported by later research.[22-24] One complicating factor is the fact that polyesters and polycarbonates can undergo ester–ester interchange reactions, especially at higher temperatures.[24-26] These reactions may lead to apparent miscibility of otherwise incompatible polymers in some cases. Another problem, which is general to the study of all polymer blends, is that the methods used to test polymer miscibility are not always unambiguous. For example, crystallization of one of the polymers during a differential scanning calorimetry scan can obscure one of the glass transitions, leading to the false impression that there is a single glass transition and the polymers are miscible.

NMR spectroscopy is a powerful tool for analysis of the microstructure of solid polymers[27-29] and can help to provide insight about the miscibility of polymer pairs such as a polyester and a polycarbonate. The NMR phenomenon of spin diffusion is an especially fruitful source of information. Spin diffusion is the process by which a perturbation of the spin system at a local site in a solid is dissipated to other sites spatially removed from the site of the initial disturbance. It occurs as a consequence of through-space dipolar interactions among nuclei. Therefore, the nuclei involved must be relatively close to each other in space if spin diffusion is to occur rapidly. Thus spin-diffusion measurements are sensitive to local structure in polymers[30-39] and have been used to check for phase separation in polymer blends in a few cases.[40-43] Another way to view spin diffusion is as a mechanism by which two nuclear reservoirs, prepared with different spin temperatures, can come into equilibrium via the dipolar coupling interactions between the individual nuclei. If each reservoir is associated with one of the components of a polymer blend, the rate at which spin transfer occurs reflects the degree of contact between the components of the polymer blend.

Measurements of spin diffusion have two parts. The spin systems involved must first be prepared with different spin temperatures. That is, the magnetization in at least one of the equilibrating reservoirs must be different from the equilibrium value. The rate at which the spin systems come into equilibrium with each other must then be de-

0024-9297/88/2221-1282$01.50/0

tected. Improvements in experimental methodology in recent years have greatly expanded the range of ways in which we can accomplish both the preparation and the observation steps in spin diffusion measurements.

New methods to measure spin diffusion within a system containing only protons illustrate the point. Proton signals of solids are typically many kilohertz broad, and the resonances from chemically different types of protons are rarely resolved in the NMR spectrum. Overlap of signals from different types of polymers in a blend generally prevents independent manipulation of the corresponding spin systems to produce different spin temperatures. Traditionally, the experimenter has had to rely on natural relaxation processes to leave the systems with different spin temperatures. Recently, it has been demonstrated that special trains of pulses and magic-angle spinning permit direct control of the spin systems in favorable cases.[37,44] Multiple-pulse trains and magic-angle spinning are also very helpful in permitting independent detection of the magnetization of the several types of protons present in a polymer blend.[43,45] The use of multiple-pulse trains requires considerable experimental finesse, however, and does not assure that the signals from the individual components of a polymer blend can be resolved anyway. A technically simpler way to monitor the magnetization of a proton system affected by spin diffusion involves transfer of the magnetization from the protons to nearby carbons, followed by measurement of signal intensities in the carbon spectrum.[46–51] Indirect detection of the progress of spin diffusion in this manner makes it possible to take advantage of the much higher inherent resolution in the carbon spectrum to observe the course of spin diffusion in the proton system.

The improvements in experimental technique are not limited to experiments directed at spin diffusion among protons, however. Spin exchange among the carbons themselves can be a useful source of information which augments the information which can be obtained from measurements of proton spin diffusion.[52–56] Carbon–carbon spin exchange is less efficient than is proton–proton spin exchange, however. Pairs of carbons involved in the process must be much closer together than would be necessary for two protons undergoing spin exchange at the same rate. Spin exchange among carbons is thus sensitive to much smaller distances than is spin exchange among protons. Unfortunately, at natural ^{13}C abundance the rate of spin exchange is too slow to compete with the rate of spin–lattice relaxation in most polymers, making observation difficult. Isotopic enrichment of polymer samples accelerates the process sufficiently to allow it to compete with spin–lattice relaxation and be useful.[56]

We have previously demonstrated the applicability of ^{13}C exchange measurements for examination of miscibility in blends of poly(ethylene terephthalate) (PET) and bisphenol A polycarbonate (BPAPC).[56] Extensive chemical reaction had almost certainly occurred in the sample used in the earlier work, however, so that the question of the inherent miscibility of the two polymers was not addressed. The purpose of the research reported here was to explore in detail whether PET is inherently miscible with BPAPC in the absence of chemical reaction between the two polymers. Miscibility at the molecular level was tested by whether carbon–carbon spin exchange could occur at a significant rate. Structure on a larger scale was explored by determination of the effect of proton spin diffusion on spin–lattice relaxation. The technique in which proton relaxation is monitored in the carbon spectrum made selective measurements of relaxation in the PET and BPAPC protons possible. The evidence based on NMR was supplemented by results of differential scanning calorimetry.

The results that we will describe indicate, in fact, that PET and BPAPC are inherently immiscible at the molecular level. A secondary stage of the work was directed at determining how chemical reaction induces molecular mixing of the initially phase-separated polymers. The emphasis of the work was on morphological changes that occur as a result of chemical reaction. Evidence as to the types of reactions involved was also obtained.

Theory

The mathematical model that best simulates proton spin diffusion depends on the morphology of the system in which spin diffusion occurs. The samples we have examined contained 20–25% polycarbonate. Because the polycarbonate concentration was relatively low, we assume that phase-separated polycarbonate existed in spherical domains. We would like to know how proton magnetization diffused out of those domains. We will see that assumption of other types of domain geometries leads to numerical predictions of the same order of magnitude as those for spheres.

An analytical expression for the magnetization concentration at any point in space at time t of a species initially confined uniformly within a sphere and diffusing from that sphere is known.[57] Calculation of the total amount of magnetization outside the sphere at time t requires integration over the magnetization concentration at each point outside the sphere. This integration is, at best, unwieldy.

Fortunately, insight into the basic problem of diffusion from a sphere can be obtained in a simple manner by consideration of diffusion of magnetization from a point source. The relevant equation is

$$C(r,t) = \frac{M}{8(\pi D t)^{3/2}} \exp(-r^2/4Dt) \tag{1}$$

where $C(r,t)$ is the concentration of magnetization at distance r from the source at time t, M is the total magnetization, and D is the diffusion constant. For spin diffusion D can be calculated from the spectral second moment.[58]

The mean-square distance $\langle d^2 \rangle$ the magnetization moves from the point source in a time t is given by

$$\langle d^2 \rangle = 4 \int_0^\infty \pi r^4 C(r,t) \, \mathrm{d}r = 6Dt \tag{2}$$

where the surface area of the sphere of radius r is used as a weighting factor in the integration. The linear average distance moved, $\langle d \rangle$, can be found with a similar integration to be $4(Dt)^{1/2}/\sqrt{\pi}$. It should be compared with the root-mean-square distance $(6Dt)^{1/2}$.

The exact expression for diffusion of magnetization out of a sphere, which we have chosen not to tackle, takes into account the fact that most of the magnetization is initially located away from the spherical center. A magnetization component located near the surface of the sphere may escape very quickly if it moves immediately toward the surface. On the other hand, it may remain in the sphere for a long time if it moves toward the center. To first order these factors compensate and the effective size of the domains that are probed by a spin-diffusion experiment is given by eq 2. We assume that when the root-mean-square distance that magnetization has moved is equal to the domain size, essentially complete equilibration of the proton magnetization from PET and from BPAPC has occurred.

Other workers have assumed a lamellar morphology for spin-diffusion calculations.[36,37,59] Spin diffusion then effectively occurs in one dimension, perpendicular to the lamellae. The mean-square distance traversed by magnetization in the one-dimensional model is $2Dt$. The root-mean-square distance in one dimension differs from that for diffusion in three dimensions (from a point source) by a factor of $\sqrt{3}$.[36,59] The value for diffusion in two dimensions, which would be appropriate for cylindrical domains, is presumably intermediate. A recent calculation of Havens and Vanderhart of diffusion from an extended source finds the mean-square distance magnetization travels from the source to be $(^4/_3)Dt$.[37] Overall there appears to be an uncertainty in distance scales of a factor of 2–3 depending upon the choice of a model. For our purposes, an uncertainty of a factor of 3 is insignificant.

We must now consider specifically how spin diffusion manifests itself experimentally. In an ideal experiment two nuclear reservoirs, which might comprise the protons in two polymers A and B, would be prepared with different spin temperatures. The equilibration of the two reservoirs as a result of exchange of magnetization would then be monitored as a function of time. The expression for the rate of magnetization transfer would be a function of the geometry and size of both the A and B domains and possibly other factors.

It is difficult to prepare the A and B spin systems directly in different temperatures without the use of multiple-pulse NMR. Instead, in the experiments referred to in this paper, the spin systems were allowed to evolve, in the traditional approach, to different temperatures as a result of nuclear relaxation. Spin diffusion was detected by how it perturbed the relaxation of the individual spin systems.

Relaxation of protons in the presence of spin diffusion can be quite complicated. Fortunately, a simplified model conveys the salient points. We assume that polymer A is the minor component of a blend and exists in isolated spheres of uniform size. Because the A protons are closer to each other than to the B protons, we assume that internal equilibrium within the A system (and likewise within the B system) is reached rapidly, whereas equilibration of the A protons with the B protons occurs at a rate determined by the size of the A domains. We write coupled differential equations for the overall rates at which the A and B magnetizations change

$$\mathrm{d}M_{\mathrm{A}}(t)/\mathrm{d}t = -(k_{\mathrm{A}} + k_{\mathrm{AB}})M_{\mathrm{A}} + k_{\mathrm{BA}}M_{\mathrm{B}} \qquad (3a)$$

$$\mathrm{d}M_{\mathrm{B}}(t)/\mathrm{d}t = k_{\mathrm{AB}}M_{\mathrm{A}} - (k_{\mathrm{B}} + k_{\mathrm{BA}})M_{\mathrm{B}} \qquad (3b)$$

where M_{A} and M_{B} are the magnetizations in the A and B reservoirs, k_{A} and k_{B} are rate constants for dissipation of magnetization from the A and B systems to the lattice (the inverses of the corresponding relaxation times), and k_{AB} and k_{BA} are the rate constants for exchange of magnetization between the A and B reservoirs. Note that $k_{\mathrm{BA}}/k_{\mathrm{AB}}$ equals K, the ratio of the number of nuclei in the A reservoir to the number of nuclei in the B reservoir.

The solution to eq 3a and 3b is

$$M_{\mathrm{A}}(t) = [M_{\mathrm{A0}} \cos^2 \phi - K^{1/2}M_{\mathrm{B0}} \sin \phi \cos \phi] \exp(R_1 t) + [M_{\mathrm{A0}} \sin^2 \phi + K^{1/2}M_{\mathrm{B0}} \sin \phi \cos \phi] \exp(R_2 t) \qquad (4a)$$

$$M_{\mathrm{B}}(t) = [-K^{1/2}M_{\mathrm{A0}} \sin \phi \cos \phi + M_{\mathrm{B0}} \sin^2 \phi] \exp(R_1 t) + [K^{1/2}M_{\mathrm{A0}} \sin \phi \cos \phi + M_{20} \cos^2 \phi] \exp(R_2 t) \qquad (4b)$$

where M_{A0} and M_{B0} are the initial magnetizations of the A and B reservoirs, $\tan^2 \phi = 2{k_{\mathrm{AB}}}^{1/2}{k_{\mathrm{BA}}}^{1/2}/(k_{\mathrm{A}} - k_{\mathrm{B}} + k_{\mathrm{AB}} - k_{\mathrm{BA}})$

$$R_1 = -(k_{\mathrm{A}} + k_{\mathrm{AB}}) \cos^2 \phi - 2(k_{\mathrm{AB}}k_{\mathrm{BA}})^{1/2} \sin \phi \cos \phi - (k_{\mathrm{B}} + k_{\mathrm{BA}}) \sin^2 \phi \qquad (5a)$$

$$R_2 = -(k_{\mathrm{A}} + k_{\mathrm{AB}}) \sin^2 \phi + 2(k_{\mathrm{AB}}k_{\mathrm{BA}})^{1/2} \sin \phi \cos \phi - (k_{\mathrm{B}} + k_{\mathrm{BA}}) \cos^2 \phi \qquad (5b)$$

When $(k_{\mathrm{AB}}k_{\mathrm{BA}})^{1/2}$ is much smaller than $k_{\mathrm{A}} - k_{\mathrm{B}}$, $\sin \phi \approx 0$, and the two decay rates are independent of each other. The rate constants R_1 and R_2 are those of the isolated individual reservoirs.

When $(k_{\mathrm{AB}}k_{\mathrm{BA}})^{1/2}$ is much larger than $k_{\mathrm{A}} - k_{\mathrm{B}}$, some algebra shows that

$$\cos^2 \phi = k_{\mathrm{AB}}/(k_{\mathrm{AB}} + k_{\mathrm{BA}})$$

$$\sin^2 \phi = k_{\mathrm{BA}}/(k_{\mathrm{AB}} + k_{\mathrm{BA}}) \qquad (6)$$

As a result

$$R_1 = -(k_{\mathrm{AB}} + k_{\mathrm{BA}})$$

$$R_2 = -k_{\mathrm{A}}\frac{k_{\mathrm{BA}}}{(k_{\mathrm{AB}} + k_{\mathrm{BA}})} - k_{\mathrm{B}}\frac{k_{\mathrm{AB}}}{(k_{\mathrm{AB}} + k_{\mathrm{BA}})} \qquad (7a)$$

If the initial ratio of the magnetization in the A and B reservoirs is K, the expressions involving R_1 drop out of eq 4a and 4b in this second case; both M_{A} and M_{B} decay with the same rate constant R_2, which is the weighted average of the decay rates for the individual reservoirs and can be rewritten

$$R_2 = {t_2}^{-1} = -{t_{\mathrm{A}}}^{-1}f_{\mathrm{A}} - {t_{\mathrm{B}}}^{-1}f_{\mathrm{B}} \qquad (7b)$$

where f_{A} and f_{B} are the relative sizes of the A and B reservoirs and can be found with a knowledge of the mole ratio of the two species and the proton content of a mole of each type and t_{A} and t_{B} are the relaxation times of the protons in the A and B systems. Note that rapid spin diffusion serves to average the relaxation properties of the systems involved.

We expect that the model described by eq 4–6 is too simplistic to fit most real relaxation curves for polymer blends affected by spin diffusion. The assumption that full equilibration of the spin system within each domain occurs rapidly compared with transfer of magnetization between domains is almost certainly wrong. Temperature gradients will be created within the domains as a result of spin diffusion into or out of each volume element. Very complicated nonexponential spin relaxation is to be expected.

The analysis also relies on the implicit assumption that the inherent relaxation time of nuclei in a given type of polymer fragment is unaffected by the intermolecular environment of that fragment; the nuclei relax at the same rate regardless of whether the polymer is surrounded by other chains of the same type or by chains of the other component of the polymer blend. The reliability of this assumption is uncertain.

Nevertheless, the model does give us a good qualitative picture of how spin diffusion affects measurements of nuclear relaxation times. Predictions based on the assumption of equal spin populations in the equilibrating reservoirs illustrate the point in the following paragraphs.

When the rate of spin diffusion (which is determined by the size of the domains containing the spin reservoirs) is small compared to the difference in the relaxation rates, each nuclear system relaxes independently. If signals from the two systems can be resolved, exponential decay of the two systems will be observed. If the signals cannot be resolved, the single observed relaxation curve will be composed of two magnetization components, the sum of which relaxes nonexponentially. If the decay constants for the signals making up the composite decay curve are sufficiently unlike, differing by a factor of 5 or so, the component decay curves can be derived from the overall signal. Otherwise the observed relaxation curve may appear to be composed of a single exponential having a decay constant intermediate to those of the actual components.

When the rate of spin diffusion is comparable to the difference in relaxation rates, the relaxation process for each species will be nonexponential, regardless of whether the NMR signals themselves are resolved or not. In other words the relaxation curves for each type of nucleus will be composed of two or more exponential curves. Once again the presence of multiple exponential decays may or may not be evident experimentally.

Observation that the proton systems associated with each polymer in a blend relax at the rates found independently for the pure polymers is a strong indication that the polymer components in the blends are separated into isolated domains unless, of course, the pure materials happen to have the same relaxation times. For the protons in each blend component to relax independently, the root-mean-square distance traversed by a typical magnetization component during the effective time of the experiment must be less than the domain size. The effective time is the inverse in the difference of magnetization rates and can be used in eq 2 for calculation of the domain size. (Here again, for illustration, we assume that the sizes of the proton reservoirs are equal.)

The inverse of the difference in spin-lattice relaxation rates of pure BPAPC and amorphous PET is 0.25 s (see below). Havens and VanderHart have provided a reasonable estimate for the diffusion constant D in PET (5.0×10^{-12} cm^2/s).[37] Equation 2 gives us a value of about 275 Å for $\langle d^2 \rangle^{1/2}$. To take into account the uncertainties in the choice of a model, we assume the effective distance range in the T_1 experiment to be 150–300 Å. We also note that in the systems actually studied the two proton reservoirs are not exactly equal in size.

The inverse difference in the relaxation rates of BPAPC (or amorphous PET) and crystalline PET is 17 ms. On resonance, the diffusion constant in the $T_{1\rho}$ experiment is scaled by $^1/_2$. Equation 2 gives an effective distance for spin diffusion between crystalline PET and amorphous BPAPC and PET in the $T_{1\rho}$ experiment to be about 51 Å. We assume a range of 30–60 Å.

The earlier paper described the basic features of carbon spin exchange in the PET/BPAPC system.[56] The effective distance scale for carbon spin exchange is less than 10 Å.

The analysis above thus demonstrates that we can examine distances in a range of a few angstroms up to a few hundred angstroms by the proper choice of experiment. Part of the goal of this work was to see the morphology of the PET/BPAPC blend change at these various distance scales as the sample was modified with heating.

Experimental Section

BPAPC with natural abundance ^{13}C is commercially available from General Electric as Lexan 145. The weight-average molecular weight used was 31 000. The glass-transition temperature, measured as the onset of the differential scanning calorimetry transition, was 145 °C.

PET used in the work had been melt polymerized to an inherent viscosity of 0.63 g/dL in phenol/chlorobenzene solution. The weight-average molecular weight was >40 000. The glass-transition temperature was 77 °C.

Polymers with ^{13}C Enrichment. The preparation of poly(ethylene terephthalate), 90% enriched with ^{13}C in the ethylene glycol moiety, has previously been reported.[60] The catalyst was a mixture of zinc acetate dihydrate and tetrabutyl orthotitanate. The glass-transition temperature was 75 °C. An amorphous sample was prepared by precipitation of 1 g of the polymer dissolved in a 3:1 mixture by volume of dichloromethane and hexafluoro-2-propanol when the solution was poured into methanol.

The BPAPC with enrichment in the carbonyl position was made from ^{13}C-labeled phosgene dissolved in benzene (Merck Isotopes). The actual concentration of phosgene in this material is less than the nominal value of 1.1 M. Determination with ^{13}C NMR of the true concentration of phosgene made possible synthesis of a polymer with much higher molecular weight than that reported before.[56] The phosgene solution was added slowly (dropwise in the final stage) to a cooled solution of 3.3 g of bisphenol A (0.0145 mol) and 2.6 g of pyridine (0.033 mol). After 30-min stirring, the solution was washed once with dilute hydrochloric acid and twice with water. The polymer precipitated when the solution was poured into isopropyl alcohol. It was collected, washed with isopropyl alcohol, and then dried under vacuum overnight at 60 °C. The yield was 3.5 g (theorectical 3.7 g). The polystyrene-equivalent number-average molecular weight was 71 300; the weight-average molecular weight was 319 000. The glass-transition temperature was 158 °C.

Polymer Blends. In a typical preparation, 0.3 g of poly(ethylene terephthalate) and 0.1 g of polycarbonate were dissolved in a mixture of 7.5 mL of hexafluoro-2-propanol and 2.5 mL of dichloromethane containing 0.08 g of sodium dihydrogen phosphate to quench any residual catalyst remaining in the PET. A coating was cast at room temperature onto glass, then was floated off in water, and dried overnight under vacuum at 130 °C. It was pressed at 270 °C for 1 min and quenched in ice water. The material with enriched PET is referred to as PET13C/PC. The blend with enriched PC is called PET/PC13C.

NMR Spectroscopy. Solid-state spectra were all acquired on a Bruker CXP-100 spectrometer equipped with a Bruker Aspect 3000 computer. The carbon frequency was 25.2 MHz. Mushoom-shaped spinners were used for magic-angle spinning. The "stem" of the mushoom was made of ceramic and contained the sample. The typical cross-polarization contact time was 1 ms. Delays between scans were 3–4 s. Proton 90° pulses were normally 4.5 μs.

Proton spin-lattice relaxation times were measured by following the recovery of the proton system after a 5-ms saturating pulse. After partial recovery the remaining magnetization was transferred to the carbon system by the standard cross-polarization technique for detection. Relaxation times in the rotating frame were determined in a similar fashion by allowing spin-locked proton magnetization partially to decay before the cross-polarization step. Relaxation times measured though the aromatic carbon signal of PET usually were more reproducible than were those measured through the carbonyl carbon signal; the values reported are those of the former.

Carbon-carbon spin exchange was detected either in a two-dimensional experiment or by following the manner in which relaxation of carbon magnetization of a nonenriched site was affected by the sign and magnitude of the magnetization established in a preparatory step at the enriched carbon site. The two-dimensional exchange spectrum provides a mapping of the exchange pathways that are active. The relaxation experiment provides a measure of the rate of cross relaxation among the carbons. Details of the procedures were described in the previous paper.[56]

Solution spectra were obtained from solutions in a 80/20 mixture of trifluoroacetic acid/deuteriomethylene chloride on a Bruker WH 500 spectrometer. The carbon frequency was 125 MHz.

Nuclear relaxation curves were simulated on a main-frame IBM 3090 computer with the help of the SAS statistical analysis package.[61] Simple exponential curves generally were fit with three independent parameters (the initial or final intensity, the exponential prefactor, and the decay constant). Nonexponential decays were simulated as the sum of two exponential functions with four independent parameters (two prefactors and two decay constants). The statistical errors reported are those given by the SAS routines.

Calorimetric measurements (differential scanning calorimetry, DSC) were performed with a Perkin-Elmer DSC II from 48 °C (below the glass transition temperature of PET) to either 260 °C (PET13C/PC) or 265 °C (PET/PC13C), these tempera-

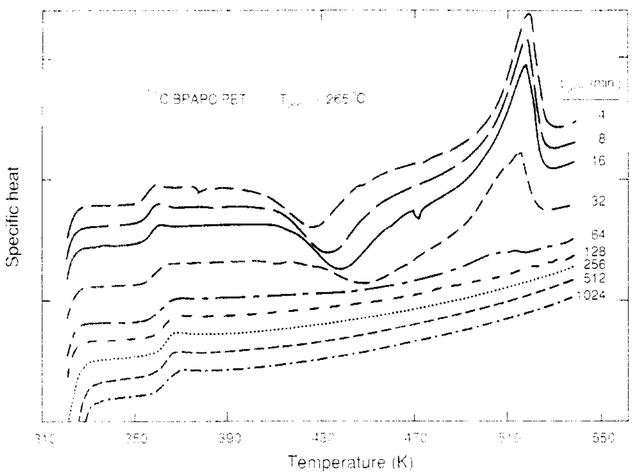

Figure 1. DSC curves for PET/PC13C after annealing at 265 °C in the calorimeter for total times indicated.

tures being slightly higher than the melting points of the PET in the respective samples. Heating rates were kept constant at 20 °C/min; samples were cooled at the fastest rates available to the instrument (approximately 50–100 °C/min). Glass-transition temperatures were taken at the onset of the transitions unless otherwise noted. The onset was defined as the intersection of lines drawn though the inflection point and though the values for the glass.

Heating of blends was done at 260 °C in an ordinary oven. Because in most practical preparations of polymer blends extrusion of polymer blends or other heat processing would occur in a normal atmosphere, no special precautions to provide isolation from the atmosphere were used. The temperature reached by a sample contained in a ceramic NMR spinner after a given time in the oven was calibrated with a thermocouple in a test sample. Within 1 min the temperature was 210 °C. Within 2 min it was 250 °C. A heating increment was 4 min unless specified otherwise. The sample was cooled in air, or in some cases, by placement of the NMR spinner in a hole in an aluminum block.

Results

Differential Scanning Calorimetry. Figure 1 shows a series of DSC traces for a sample of PET/PC13C that was annealed in the calorimeter at 265 °C between each scan. The curves show three primary features for the samples that had been annealed a total time of 30 min or less: a glass transition between 77 and 93 °C, a crystallization exotherm at about 155 °C, and a melting transition at 243 °C. The exotherm moved to higher temperatures and broadened each time the sample was annealed. With repeated heatings it eventually disappeared. The large melting peak moved to lower temperature, broadened, and also went away after repeated annealings. The glass-transition region moved to higher temperature. In none of the curves is there evidence of a glass transition for phase-separated BPAPC, but the large exotherm that occurs for samples that have been annealed only short times obscures the region in which the glass transition of BPAPC would occur.

The changes in the temperature of the observed glass transition of PET13C/PC are shown schematically in Figure 2. Figure 3 shows a comparable plot for PET/PC13C. The observed glass-transition temperature of PET13C/PC reached 89–92 °C after about 200 min of annealing. Figure 2 gives some indication that a plateau was eventually reached. By contrast, the glass-transition temperature of PET/PC13C was only 87 °C after 1000 min and still appeared to be climbing each time the sample was annealed.

NMR Spectroscopy. Pure Polymers. For BPAPC the proton $T_{1\rho}$ value, measured though the carbons, was 5.54 ± 0.06 ms. The T_1 was 0.19 ± 0.01 s.

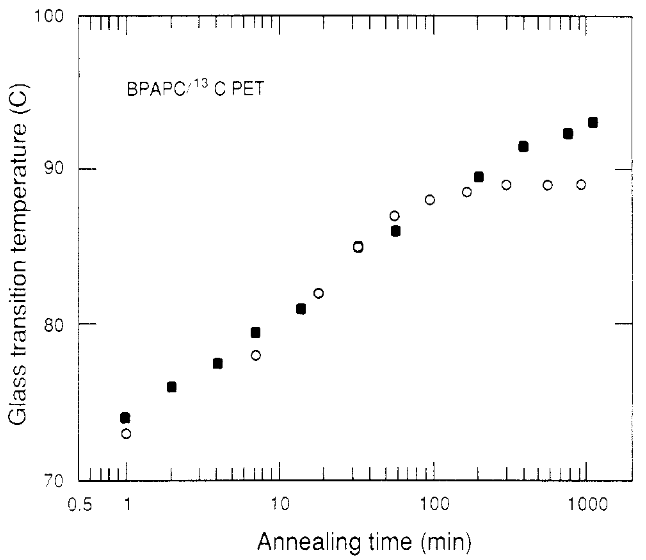

Figure 2. Changes in the glass-transition temperature observed for two samples of PET13C/PC, heated in the calorimeter as indicated in Figure 1. The two symbols indicate results from two identically prepared samples. The T_g values are the temperatures at the onset of the transition region.

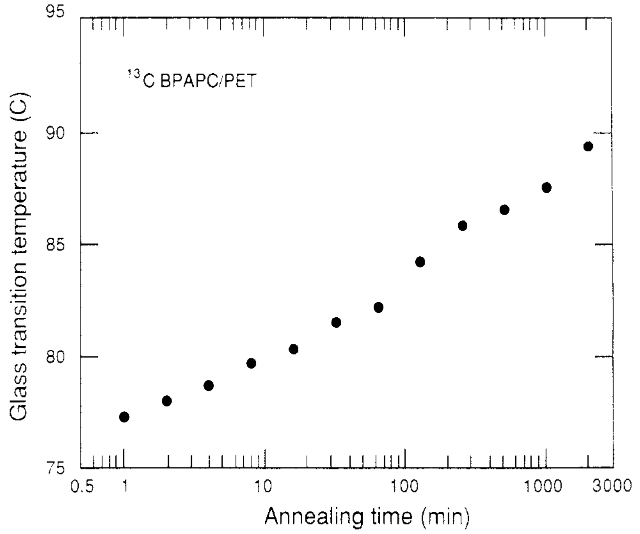

Figure 3. Changes in the glass-transition temperature observed for PET/PC13C, heated as indicated in Figure 1.

The results were more complicated for PET. For the ^{13}C-labeled material, precipitated as an amorphous polymer, the $T_{1\rho}$ and T_1 values, respectively, were 4.18 ± 0.03 ms and 0.67 ± 0.01 s. By contrast, nonexponential $T_{1\rho}$ relaxation was observed for a crystalline, nonenriched sample. The relaxation curve was decomposed into two exponential components. The fast-relaxing component comprised 24% of the initial intensity and had a time constant of 4.7 ± 1.8 ms. The slowly relaxing component comprised 76% of the initial intensity and had a time constant of 27.4 ± 2.5 ms. Havens and VanderHart also found that the proton $T_{1\rho}$ relaxation of partially crystalline PET was nonexponential, but they observed that only 60% of the initial intensity relaxed slowly.[37] The discrepancy between their results and ours probably results from the fact that they determined the proton relaxation behavior directly through the proton spectrum, whereas we made indirect measurements through the carbon spectrum.

We previously reported a ^{13}C spin–lattice relaxation time of the carbonyl carbon in BPAPC of 6.0 ± 0.6 s at a carbon frequency of 25.2 MHz.[56] The spin–lattice relaxation time

Table I
Proton Spin-Lattice Relaxation Times (T_1) for PET13C/PC

total heating time, min	T_1, s BPAPC[a]	PET[b]
0	0.18 ± 0.03	0.74 ± 0.06
3	0.24 ± 0.03	1.2 ± 0.2
9	0.28 ± 0.03	1.0 ± 0.1
27	0.37 ± 0.04	0.39 ± 0.03

[a] Measured through the carbonyl carbon signal. Some values are averages of multiple determinations. [b] Measured through the aromatic carbon signal.

of the methylene carbons in PET was 7.7 ± 0.6 s.[56]

PET13C/PC. The proton spin-lattice relaxation times, T_1, measured though the carbon spectrum after several cycles of heating and slow cooling in the NMR spinner are shown in Table I. Before the sample was heated, the protons of PET and BPAPC had clearly different spin-lattice relaxation times of 0.74 and 0.18 s, respectively. The first heating step produced a significant jump in the relaxation time of the PET protons but a much smaller increase in the relaxation times of the BPAPC protons. Further heating resulted in a fall of the PET relaxation times. After 27 min of heating the relaxation times for the two polymers were equal.

Initially, the spin-lattice relaxation time in the rotating frame, $T_{1\rho}$, of PET was 3.8 ± 0.01 ms and that of BPAPC was 4.5 ± 0.02 ms. With heating the apparent relaxation time of the PET rose to over 10 ms. Unfortunately, phase instabilities in the proton channel of the spectrometer at the time the work on this blend was done prevented accurate measurement of proton $T_{1\rho}$ values over 10 ms, so an exact value was not obtained. After 27 min of heating the $T_{1\rho}$ values of both polymers were about 4.2 ms.

In the absence of close molecular contact between the two polymers in a blend, carbon spin exchange should not occur, and the decay of longitudinal magnetization from the carbons in one of the polymers should be independent of the spin state in which the carbons of the other polymer is prepared. The decay time of the BPAPC carbonyl carbon of PET13C/PC was 5.1 ± 0.7 s before the sample was annealed in the NMR spinner, even when the labeled carbon was prepared with magnetization of opposite sign from that of the carbonyl carbon. The observed value is close to the value of 6.0 ± 0.6 s observed for pure BPAPC. Apparently spin diffusion between the labeled ethylene carbons of PET and the carbonyl carbon of BPAPC does not occur prior to annealing in the NMR spinner.

After 3 min heating the apparent ^{13}C relaxation time of the BPAPC carbonyl carbon when the labeled PET carbon had magnetization of opposite sign was 2.8 ± 0.3 s; some spin diffusion may have occurred. After 27 min of annealing time it was 0.4 ± 0.1 s, close to the apparent relaxation time seen before in a sample in which extensive chemical reaction had occurred.[56]

The occurrence of carbon-carbon spin exchange in the sample which had been heated 27 min was checked with a two-dimensional exchange experiment. Spin exchange is indicated in the two-dimensional results by a "cross peak" off the diagonal of the spectrum. Figure 4 shows such a cross peak between the PET labeled methylene carbons and the BPAPC carbonyl carbon, confirming that spin exchange does occur in the heated sample during a time of 400 ms. There are also cross peaks resulting from spin exchange between the PET methylenes and the PET aromatic and carbonyl carbons. Figure 5 shows a cross section taken from the two-dimensional spectrum through the cross peaks. The intensity of the BPAPC cross peak is about 25% that of the PET cross peaks.

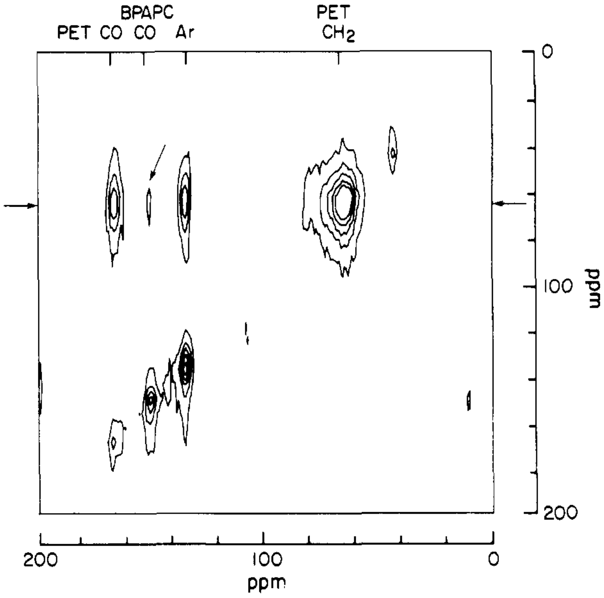

Figure 4. Two-dimensional ^{13}C spin-exchange spectrum for PET13C/PC after it was heated in four steps for 27 min. The arrow marks the exchange peak.

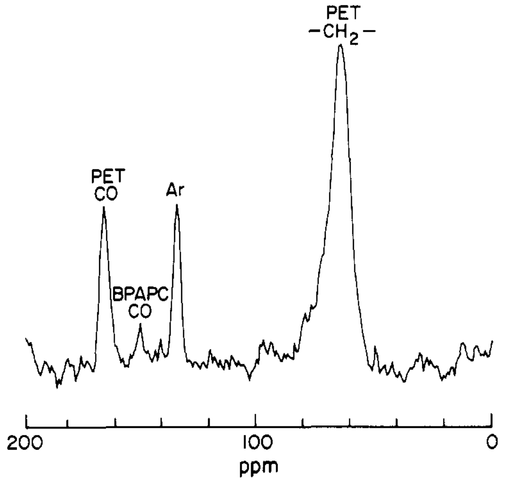

Figure 5. Slice from the spectrum in Figure 4 at the position indicated showing the signals of the PET and BPAPC carbons in contact with the labeled ethylene glycol PET carbons.

PET/PC13C. The behavior of the proton spin-lattice relaxation times of the PET and BPAPC as the sample was heated is shown in Figure 6. As was the case for PET13C/PC, heating first caused a steep increase in the T_1 of PET, followed by a gradual decline.

The BPAPC relaxation time initially was the same as that of pure BPAPC and remained at the same value for the first two heatings. The high values of T_1 measured after the third to fifth heatings may be anomalous; the relaxation time dropped again to a low value after the next two heatings. A smooth increase in the relaxation time of the BPAPC protons and a decrease in the relaxation time of the PET occurred as the sample was heated further. Ultimately, the relaxation times of the protons in PET and those in BPAPC approached the same value.

The proton $T_{1\rho}$ values of the PET and BPAPC protons in PET/PC13C were initially almost the same (Figure 7), and the relaxation time of the BPAPC protons changed only slightly as the sample was heated. The relaxation curve of the PET protons became nonexponential after the sample had been heated, however. As was the case for pure PET, the decay curve was decomposed into slow and fast components; the time constant of the fast component is

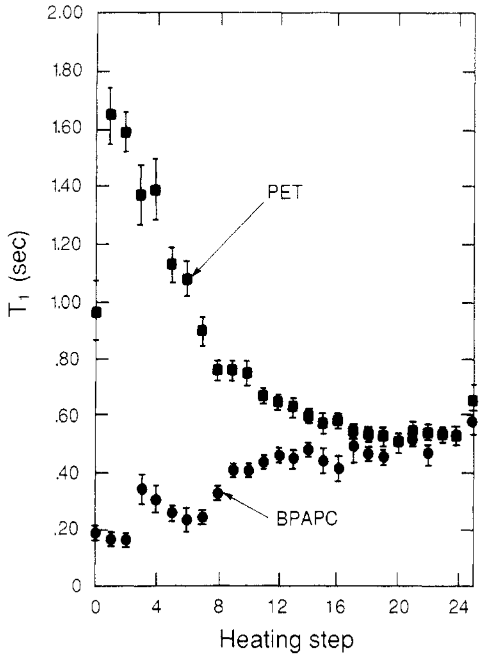

Figure 6. Proton spin-lattice relaxation times, T_1, measured from the carbon spectrum of PET/PC13C as a function of the number of times the sample was heated at 260 °C and allowed to cool in air or a metal block. The upper trace is for PET; the lower trace is for BPAPC. The error bars are the standard deviations calculated in the fit of the relaxation curves.

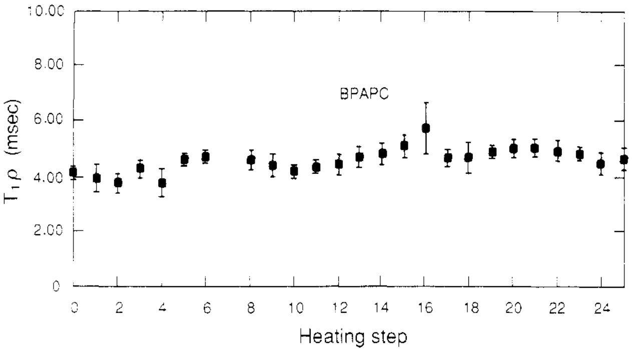

Figure 7. Proton spin-lattice relaxtion times $T_{1\rho}$ for BPAPC in PET/PC13C as a function of the number of times the sample was heated and cooled (see Figure 6).

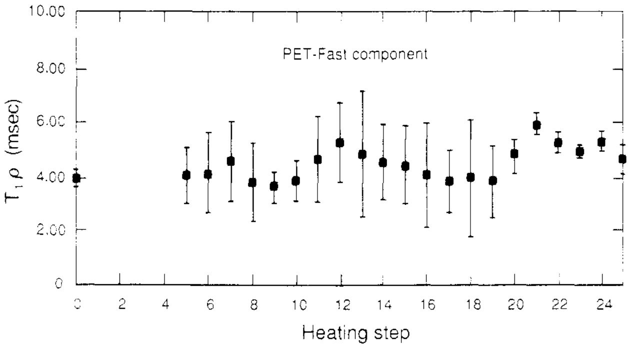

Figure 8. Proton spin-lattice relaxation times $T_{1\rho}$ for PET (fast-relaxing component) in PET/PC13C as a function of the number of times the sample was heated and cooled (see Figure 6). The fast-relaxing component was no longer separated from the slowly relaxing component after the 20th healing.

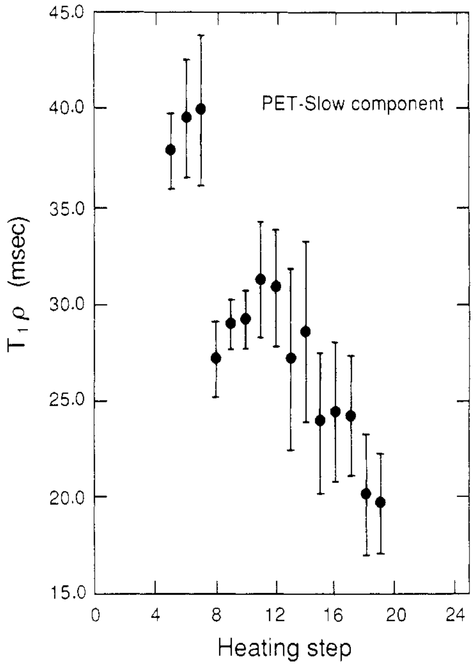

Figure 9. Proton spin-lattice relaxation time $T_{1\rho}$ (slowly relaxing long component) for PET in PET/PC13C as a function of the number of times the sample was heated and cooled (see Figure 6). After the 20th heating the fast and slowly relaxing components of PET could no longer be separated.

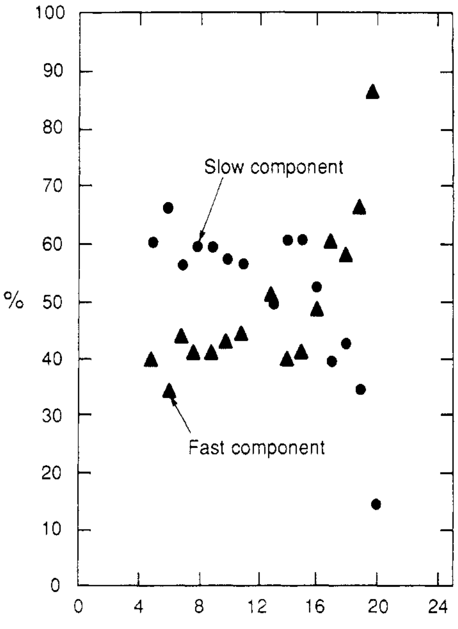

Figure 10. Apparent percentage of fast-relaxing protons (those having a long $T_{1\rho}$) (circles) and slowly relaxing protons (those having a short $T_{1\rho}$) (x's) in PET as a function of the number of times the sample was heated. After 20 heatings there was too little of the slowly relaxing component for its signal to be resolved.

plotted in Figure 8 and that of the slow component is plotted in Figure 9. The relative sizes of the two components as a function of time was plotted in Figure 10. The relaxation time of the fast component was essentially the same as that of the PET protons in the unheated material and was unchanged by subsequent heating steps. The relaxation time of the slow component (Figure 9) was initially about 40 ms and gradually decreased as the sample was heated.

The apparent percentage of the slowly relaxing component held steady until after the 14th heating (Figure 10). After the 20th heating only the fast-relaxing component could be detected. The continued presence of small amounts of the fast-relaxing component could be detected indirectly after the 20th heating by a slight elevation of the observed relaxation time of the magnetization as a

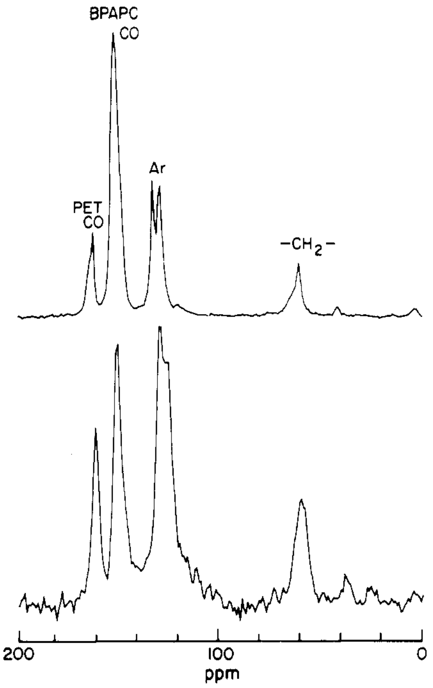

Figure 11. Carbon spectra of PET/PC13C taken with high-power proton decoupling and magic-angle spinning after (a) the 9th heating (top) and (b) the 25th heating (bottom). The loss of intensity of the BPAPC carbonyl signal at 175 ppm relative to the other signals in the lower spectrum should be noted.

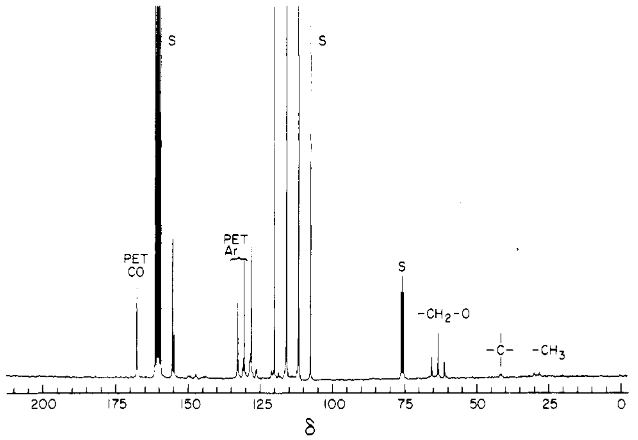

Figure 12. High-resolution ^{13}C NMR spectrum of a solution of PET/PC13C in deuteriated trifluoroacetic acid, taken after the 25th heating and cooling cycle.

whole (as shown by the last five points in Figure 8).

Figure 11 shows the actual ^{13}C NMR spectra of the solid recorded after the 9th and 25th heatings. The most obvious difference of the latter spectrum from the former is that the intensity of the BPAPC carbonyl was drasticaly reduced relative to that of the other carbons by heating. That the ethylene glycol signal of the solid heated samples is composed of at least three peaks can be established with solution ^{13}C NMR spectroscopy. The spectrum of a sample extracted into trifluoroacetic acid from the heated blend is shown in Figure 11. Some material in the heated blend was insoluble, however, and the solution spectrum contains only small signals from the bisphenol A fragments.

Discussion

Several pieces of evidence indicate that both PET13C/PC and PET/PC13C consist after preparation of phase-separated, amorphous PET and BPAPC. For example, the proton T_1 values in the starting materials were the same as those of the pure, amorphous polymers. Likewise, the observed glass-transition temperature for PET/PC13C was initially close to that of pure PET.

There was no sign that the proton T_1 relaxation of the PET and the BPAPC in the starting material were even partially averaged together by spin diffusion. The analysis earlier in the paper allows us to conclude that the BPAPC domains in the initially prepared material averaged at least 150–300 Å in size.

Nevertheless, we must be cautious in deciding that PET and BPAPC are inherently immiscible. In blends cast from solvent, phase separation of miscible polymers can occur if the solvent interacts more strongly with one of the polymers than with the other (the "$\Delta\chi$ effect").[62] The subsequent melting and quenching of the samples was designed to counteract solvent effects, but most miscible polymer pairs have a lower critical-solution temperature.[63] It is possible that the heating process itself led to phase separation in the system as it was initially prepared. Our data effectively indicate that PET and BPAPC are immiscible at about 260 °C.

Heating of PET13C/PC and PET/PC13C in the NMR spinner above the melting point of PET, followed by relatively slow cooling, produced crystalline PET, as was indicated by the longer T_1 value for the PET protons after heating and by the appearance of a slowly relaxing component of the $T_{1\rho}$ magnetization. The DSC results also showed that elevated temperature induces crystallization of PET in the blends. Crystallization of PET in blends with BPAPC has been previously noted.[24,64]

The crystalline regions were, of course, phase separated from the BPAPC. The polymers could still have been mixed in the amorphous regions of the partially crystalline blends, but a simple calculation suggests otherwise, at least for PET/PC13C. The calculation requires knowledge of the degree to which the PET was crystallized. The apparent crystallinity shown by Figure 10 is not reliable because it is measured indirectly though the carbon spectrum, and the values obtained for pure PET by the indirect method are much larger than those found directly from the proton spectrum.[37] For the calculation we thus assume that 50% of the PET was crystalline. We also assume that the PET crystals were isolated from the BPAPC protons, either because they were large or because they were surrounded by amorphous PET.

If there were complete mixing of the PET and the BPAPC in the amorphous regions, 61% of the protons in those regions would belong to PET and 39% would belong to BPAPC. With the help of eq 7b we calculate that the average T_1 value of protons in a amorphous region would be 0.35 s.

Figure 6 shows that the T_1 value of the BPAPC protons in PET/PC13C remained close to the value for pure BPAPC for three heating and cooling cycles. Heating did not appear to lead immediately to complete mixing in the amorphous regions of this sample. Ultimately, of course, complete mixing does occur, as is indicated by the fact that the proton NMR relaxation times of the blend components ultimately approach the same value.

Overall we conclude that PET and BPAPC are not inherently miscible, at least at 260 °C, but that miscibility is induced by chemical reaction between the polymers. Recent work by other authors supports the conclusion that unreacted PET and BPAPC are immiscible.[22,24,64]

Ester–ester interchange, which occurs in both pure PET[65,66] and pure BPAPC,[67] is a possible compatibilizing reaction, although other reactions are also possible. In the next few paragraphs we will discuss some aspects of the chemistry which may occur in the PET/BPAPC system, and we will then analyze the effect the chemistry has on the blend morphology.

Chemical reactivity in blends of poly(butylene terephthalate) and bisphenol A polycarbonate has been studied extensively.[23,25,68–72] Only very recently have reports on the chemistry of the PET/BPAPC system appeared.[26,73,74] It appears that as many as seven different reactions are possible, including the formation of diaryl, dialkyl, and aryl alkyl ethers. Each of the ethers is formed with the loss of carbon dioxide originating in the carbonate group of BPAPC. Previous workers demonstrated that carbon dioxide was formed when a mixture of PET and BPAPC was heated but could not determine whether the BPAPC carbonate group was the source of the gas. Figure 11 shows that, at least in PET/PC13C, the carbonyl intensity decreased as the sample was heated repeatedly above the PET melting point.

The solution NMR spectrum shows that a number of the other chemical moieties in the blends were also changed by chemical reaction as well. In particular, the ethylene glycol group was clearly affected by reaction, as indicated by the multiple peaks in the solution NMR spectrum of the final material. The primary purpose of the present work was, however, to elucidate the morphological effects of chemical reaction on the PET/BPAPC system. The details of the chemistry involved are assumed to be basically the same as those described in the literature.[73,74]

The relative importance of the various possible reactions may, however, have been different for PET13C/PC than for PET/PC13C. The reactivity of polyesters is known to be quite sensitive to the nature of catalysts present, titanium compounds being especially effective in promoting ester–ester interchange.[26,58] The ^{13}C-labeled PET used in PET13C/PC is relatively rich in titanium catalyst; commercial PET is made with a minimum of catalyst. Thus PET13C/PC probably is more reactive than is PET/PC13C to ester–ester interchange, even though the activity of the catalyst has presumably been reduced by the presence of sodium dihydrogen phosphate in the sample. Other reactions not requiring the catalyst may be more important in the other sample. Nevertheless, neither sample is inactive. In the absence of the metal catalyst even free carboxylic acid end groups may catalyze some reactions[66] and partial hydrolysis of the polymers may also play a role as water was not completely excluded.[75]

We are now ready to return to the discussion of the morphology of the blends. Crystalline PET continued to be formed to about the same extent in PET/PC13C after each heating until the process had been repeated over 15 times. Each time the sample was heated; however, the relative size of the crystalline domains appears to have decreased; both the PET proton T_1 and $T_{1\rho}$ values decreased at each heating step. A small amount of chemical reaction does not interfere with the overall ability of the PET to crystallize but does restrict the size of the crystalline domains.

At least some of the crystalline PET domains which were formed after the fifth heating were smaller than 30–60 Å because the $T_{1\rho}$ as well as the T_1 values were disturbed by the heating process. The relaxation times of the crystalline PET were partly averaged with those of the amorphous PET and the BPAPC. We may conclude that some of the phase-separated domains of amorphous BPAPC were smaller than 150–300 Å because the proton T_1 values of BPAPC change at each heating step. Presumably the sites of ester interchange in the reacted polymers form the phase boundaries between PET and BPAPC domains.

Eventually, after more than 15 heating steps in the case of PET/PC13C, blocks of pure PET no longer were present in sufficient concentration for crystallization to take place as the molten sample cooled. Likewise, after multiple heatings the crystallization exotherm in the DSC no longer appeared (Figure 1). The apparent crystallinity of the sample dropped rapidly after the 15th heating step (Figure 10). In the case of PET13C/PC, chemical reaction ultimately resulted in a sample in which the chemical moieties from PET and BPAPC were mixed at the molecular level. The slice from the two-dimensional carbon-13 spin exchange spectrum shown in Figure 5 shows that the ratio of the number of PET aromatic carbons in contact with the PET ethylene glycol carbons to the number of BPAPC carbons is about the same as the ratio of such carbons present in the system. Carbon–carbon spin exchange in PET/PC13C was not observed, even in the highly reacted sample, but this may simply reflect the fact that the labeled carbon was lost from the system as reaction proceeded.

An important question in the PET/BPAPC system, as well as in any mixture of polymers which have the potential to react together, is just how much reaction must occur before the system becomes homogeneous? Extensive chemical reaction between PET and BPAPC ultimately produces a random copolymer. A system without phase separation likely occurs long before the polymers have been completely randomized, however. Theoretical work has consistently predicted that the critical block size at which phase separation occurs in block copolymers is much larger than the critical polymer size at which phase separation occurs in mixtures of pure polymers.[76–79] Thus we might expect that relatively small amounts of reaction might lead to phase mixing in systems in which intermolecular interactions are not too unfavorable.

Consider for a moment the effect of chemical reaction on a mixture initially consisting of two homopolymers whose chains all contain the same number of monomer units. Breakage of each of the chains at three equally spaced sites produces blocks with $^1/_4$ the number-averaged monomer units. This fact, combined with an increased tendency of block copolymers as opposed to pure polymers to form homogeneous systems may mean that surprisingly small amounts of reaction may induce homogeneity in a blend.

Real systems, of course, will be much more complicated than is indicated by the model described above. Even in a phase-separated system, rather diffuse phase boundaries in which extensive polymer mixing occurs are likely to occur. Nevertheless, we think it is important to consider that even small amounts of chemical reaction can homogenize a system of immiscible polymers.

Conclusions

In the absence of chemical reaction mixtures of PET and BPAPC appear to be immiscible. Successive cycles of melting followed by cooling in the air or in a metal block induce crystallization in the PET regions. After repeated heating steps the crystals are formed to the same overall extent as after a single heating but are smaller. Extensive heating steps eventually prevent the formation of PET crystals at all and results in a homogeneous system. The chemical reactions resulting in polymer homogenization include a loss of the BPAPC carbonyl group.

Acknowledgment. We are very grateful to Mr. Hans Grashof for preparation of the ^{13}C-enriched PET and to Ms. Jeanne Kaeding for synthesis of the enriched BPAPC. Ms. Julie Machell prepared some of the blended films.

Registry No. PET, 25038-59-9; BPAPC (SRU), 24936-68-3; BPAPC (copolymer), 25037-45-0.

References and Notes

(1) ten Brinke, G.; Karasz, F. E.; MacKnight, W. J. *Macromolecules* **1983**, *16*, 1827.
(2) Kambour, R. P.; Bendler, J. T.; Bopp, R. C. *Macromolecules* **1983**, *16*, 753.
(3) Paul, D. R.; Barlow, J. W. *Polymer* **1984**, *25*, 487.
(4) Balazs, A. C.; Sanchez, I. C.; Epstein, I. R.; Karasz, F. E.; MacKnight, W. J. *Macromolecules* **1985**, *18*, 2188.
(5) Balazs, A. C.; Karasz, F. E.; MacKnight, W. J.; Ueda, H.; Sanchez, I. C. *Macromolecules* **1985**, *18*, 2784.
(6) Cantow, J.-J.; Schulz, O. *Polym. Bull. (Berlin)* **1986**, *15*, 449.
(7) Shiomi, T.; Karasz, F. E.; MacKnight, W. J. *Macromolecules* **1986**, *19*, 2274, 2645.
(8) Wahmund, D. C.; Paul, D. R.; Barlow, J. W. *J.* Appl. *Polym. Sci.* **1978**, *22*, 2155.
(9) Nassar, T. R.; Paul, D. R.; Barlow, J. W. *J. Appl. Polym. Sci.* **1979**, *23*, 85.
(10) Makarewicz, P. J.; Wilkes, G. L. *J. Appl. Polym. Sci.* **1979**, *23*, 1619.
(11) Mohn, R. N.; Paul, D. R.; Barlow, J. W.; Cruz, C. A. *J. Appl. Polym. Sci.* **1979**, *23*, 575.
(12) Mondragon, I.; Cortazar, M.; Guzman, G. M. *Makromol. Chem.* **1983**, *184*, 1741.
(13) Singh, R. K. *J. Polym. Mater.* **1984**, *1*, 230.
(14) Avakian, R. W.; Allen, R. B. *Polym. Eng. Sci.* **1985**, *25*, 462.
(15) Smith, W. A.; Barlow, J. W.; Paul, D. R. *J. Appl. Polym. Sci.* **1981**, *26*, 4233.
(16) Masi, P.; Paul, D. R.; Barlow, J. W. *J. Polym. Sci., Polym. Phys. Ed.* **1982**, *20*, 15.
(17) Joseph, E. A.; Lorenz, M. D.; Barlow, J. W.; Paul, D. R. *Polymer* **1982**, *23*, 112.
(18) Barnum, R. S.; Barlow, J. W.; Paul, D. R. *J. Appl. Polym. Sci.* **1982**, *27*, 4065.
(19) Joseph, E. A.; Paul, D. R.; Barlow, J. W. *J. Appl. Polym. Sci.* **1982**, *27*, 4807.
(20) Preston, W. E.; Barlow, J. W.; Paul, D. R. *J. Appl. Polym. Sci.* **1984**, *29*, 845, 2251.
(21) Murff, S. R.; Barlow, J. W.; Paul, D. R. *J. Appl. Polym. Sci.* **1984**, *29*, 3231.
(22) Chen, X.-Y.; Birley, A. W. *Br. Polym. J.* **1985**, *17*, 347.
(23) Hanrahan, B. D.; Angeli, S. R.; Runt, J. *Polym. Bull. (Berlin)* **1986**, *14*, 399.
(24) Hanrahan, B. D.; Angeli, S. R.; Runt, J. *Polym. Bull. (Berlin)* **1986**, *15*, 455.
(25) Birley, A. W.; Chen, X. Y. *Br. Polym. J.* **1984**, *16*, 77.
(26) Pilati, F.; Marianucci, E.; Berti, C. J. *J. Appl. Polym. Sci.* **1985**, *30*, 1267.
(27) Assink, R. A. *Macromolecules* **1978**, *11*, 1233.
(28) McBrierty, V. J. *Faraday Discuss. Chem. Soc.* **1979**, *No. 68*, 78.
(29) McBrierty, V. J.; Douglass, D. C. *Macromol. Rev.* **1981**, *16*, 295.
(30) Cheung, T. T. P.; Gerstein, B. C. *J. Appl. Phys.* **1981**, *52*, 5517.
(31) Cheung, T. T. P. *Phys. Rev. A* **1981**, *23*, 1404.
(32) Cheung, T. T. P. *J. Chem. Phys.* **1982**, *76*, 1248.
(33) Packer, K. J.; Pope, J. M. *J. Magn. Reson.* **1983**, *55*, 378.
(34) Cudby, M. E. A.; Packer, K. J.; Hendra, P. J. *Polym. Commun.* **1984**, *25*, 303.
(35) Nierzwicki, W. J. *J. Appl. Polym. Sci.* **1984**, *29*, 1203.
(36) Packer, K. J.; Pope, J. M.; Yeng, R. R.; Cudby, M. E. A. *J. Polym. Sci., Polym. Phys. Ed.* **1984**, *22*, 589.
(37) Havens, J. R.; VanderHart, D. L. *Macromolecules* **1985**, *18*, 1663.
(38) Tanaka, H.; Nishi, T. *Phys. Rev. B: Condens. Matter* **1986**, *33*, 32.
(39) Tanaka, H.; Nishi, T. *J. Appl. Phys.* **1986**, *59*, 1488.
(40) Kwei, T. K.; Nishi, T.; Roberts, R. F. *Macromolecules* **1974**, *7*, 667.
(41) McBrierty, V. J.; Douglass, D. C.; Kwei, T. K. *Macromolecules* **1978**, *11*, 1265.
(42) Albert, B.; Jerome, R.; Teyssie, P.; Smyth, G.; McBrierty, V. J. *Macromolecules* **1984**, *17*, 2552.
(43) Caravatti, P.; Neuenschwander, P.; Ernst, R. R. *Macromolecules* **1985**, *18*, 119.
(44) Caravatti, P.; Levitt, M. H.; Ernst, R. R. *J. Magn. Reson.* **1986**, *68*, 323.
(45) Lind, A. C. *J. Chem. Phys.* **1977**, *66*, 3482.
(46) Stejskal, E. O.; Schaefer, J.; Sefcik, M. D.; McKay, R. A. *Macromolecules* **1981**, *14*, 275.
(47) Zumbulyadis, N. *J. Magn. Reson.* **1983**, *53*, 486.
(48) Kaplan, S. *Polym. Prepr. (Am. Chem. Soc., Div. Polym. Chem.)* **1984**, *25*, 356.
(49) Cudby, M. E. A.; Harris, R. K.; Metcalfe, K.; Packer, K. J.; Smith, P. W. R.; Bunn, A. *Polymer* **1985**, *26*, 169.
(50) Tekely, P.; Laupetre, F.; Monnerie, L. *Polymer* **1985**, *26*, 1081.
(51) Kitamaru, R.; Horii, F.; Murayama, K. *Macromolecules* **1986**, *19*, 636.
(52) Virlet, J.; Ghesquieres, D. *Chem. Phys. Lett.* **1980**, *73*, 323.
(53) Caravatti, P.; Deli, J. A.; Bodenhausen, G.; Ernst, R. R. *J. Am. Chem. Soc.* **1982**, *104*, 5506.
(54) Szeverenyi, N. M.; Sullivan, M. J.; Maciel, G. E. *J. Magn. Reson.* **1982**, *47*, 462.
(55) Edzes, H. T.; Bernards, J. P. C. *J. Am. Chem. Soc.* **1984**, *106*, 1515.
(56) Linder, M.; Henrichs, P. M.; Hewitt, J. M.; Massa, D. J. *J. Chem. Phys.* **1985**, *82*, 1585.
(57) Carslaw, H. S.; Jaeger, J. C. *Conduction of Heat in Solids*; Oxford: New York, 1959.
(58) Abragam, A. *The Principles of Nuclear Magnetism*; Oxford: New York, 1961; p 138.
(59) Cheung, T. T. P.; Gerstein, B. C.; Ryan, L. M.; Taylor, R. E.; Dybowski, D. R. *J. Chem. Phys.* **1980**, *73*, 6059.
(60) Henrichs, P. M.; Linder, M.; Hewitt, J. M.; Massa, D.; Isaacson, H. V. *Macromolecules* **1984**, *17*, 2412.
(61) SAS Institute Inc., Box 8000, Cary, NC.
(62) Robard, A.; Patterson, D. G. *Macromolecules* **1977**, *10*, 706.
(63) Paul, D. R.; Newman, S. *Polymer Blends*; Academic: New York, 1978.
(64) Jo, W. H.; Kim, S. D. *Polymer (Korea)* **1985**, *9*, 537.
(65) McAlea, K. P.; Schultz, J. M.; Gardner, K. H.; Wignall, G. D. *Polymer* **1986**, *27*, 1581.
(66) Droscher, M.; Schmidt, F. G. *Polym. Bull. (Berlin)* **1981**, *4*, 261.
(67) Ballard, D. G. H.; Burgess, A. N.; Cheshire, P.; Janke, E. W.; Nevin, A.; Schelten, J. *Polymer* **1981**, *22*, 1353.
(68) Devaux, J.; Godard, P.; Mercier, J. P. *Polym. Eng. Sci.* **1982**, *22*, 229.
(69) Devaux, J.; Godard, P.; Mercier, J. P. *J. Polym. Sci., Polym. Phys. Ed.* **1982**, *20*, 1875.
(70) Devaux, Godard, P.; Mercier, J. P.; Touillaux, R.; Dereppe, J. M. *J. Polym. Sci., Polym. Phys. Ed.* **1982**, *20*, 1881.
(71) Devaux, J.; Godard, P.; Mercier, J. P. *J. Polym. Sci., Polym. Phys. Ed.* **1982**, *20*, 1895.
(72) Devaux, J.; Godard, P.; Mercier, J. P. *J. Polym. Sci., Polym. Phys. Ed.* **1982**, *20*, 1901.
(73) Huang, Z. H.; Wang, L. H. *Makromol. Chem., Rapid Commun.* **1986**, *7*, 255.
(74) Godard, P.; Dekoninck, J. M.; Devlesaver, V.; Devaux, J. *J. Polym. Sci., Polym. Chem. Ed.* **1986**, *24*, 3301, 3315.
(75) Schilling, F. C.; Ringo, W. M., Jr.; Sloane, N. J. A.; Bovey, F. A. *Macromolecules* **1981**, *14*, 532.
(76) Meier, D. J. *J. Polym. Sci., Part C* **1969**, *26*, 81.
(77) Krause, S. *Macromolecules* **1970**, *3*, 84.
(78) Leibler, L. *Macromolecules* **1980**, *13*, 1602.
(79) Helfand, E. *Acc. Chem. Res.* **1975**, *8*, 295.